

Article pubs.acs.org/JACS

A General DNA-Gated Hydrogel Strategy for Selective Transport of **Chemical and Biological Cargos**

Yuwei Gu, Max E. Distler, Ho Fung Cheng, Chi Huang, and Chad A. Mirkin*



Cite This: J. Am. Chem. Soc. 2021, 143, 17200-17208



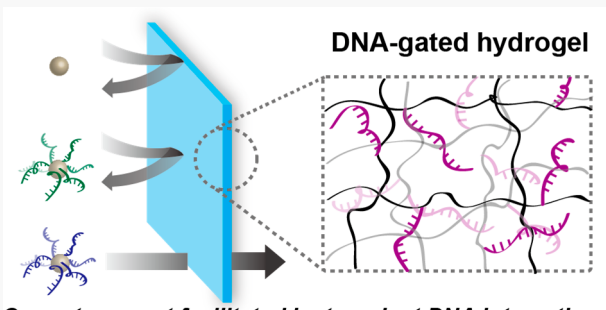
ACCESS I

Metrics & More

Article Recommendations

Supporting Information

ABSTRACT: The selective transport of molecular cargo is critical in many biological and chemical/materials processes and applications. Although nature has evolved highly efficient in vivo biological transport systems, synthetic transport systems are often limited by the challenges associated with fine-tuning interactions between cargo and synthetic or natural transport barriers. Herein, deliberately designed DNA-DNA interactions are explored as a new modality for selective DNA-modified cargo transport through DNA-grafted hydrogel supports. The chemical and physical characteristics of the cargo and hydrogel barrier, including the number of nucleic acid strands on the cargo (i.e., the cargo valency) and DNA-DNA binding strength, can be used to regulate the efficiency of cargo transport.



Cargo transport facilitated by transient DNA interactions

Regimes exist where a cargo-barrier interaction is attractive enough to yield high selectivity yet high mobility, while there are others where the attractive interactions are too strong to allow mobility. These observations led to the design of a DNA-dendron transport tag, which can be used to universally modify macromolecular cargo so that the barrier can differentiate specific species to be transported. These novel transport systems that leverage DNA-DNA interactions provide new chemical insights into the factors that control selective cargo mobility in hydrogels and open the door to designing a wide variety of drug/probe-delivery systems.

■ INTRODUCTION

Processes critical to chemical and materials applications, such as controlled release, ¹⁻⁴ (bio)chemical sensing, ^{5,6} heterogeneous catalysis, ^{7,8} and molecular separation, ^{9,10} rely on understanding and controlling molecular transport. Many synthetic transport systems distinguish cargo based on size, 11-13 and these systems often have poor selectivity when the size difference between the target and non-target species is not sufficiently large, as is often the case for (bio)macromolecule cargo. Some synthetic selective transport systems employ semi-permeable barriers, which operate following molecular selection mechanisms based on affinity interactions and allow only target cargo to pass through. In particular, cargo-barrier interactions have been maximized or minimized in applications where controlled transport is critical, such as protein purification using affinity tags, 14 pollutant adsorption in porous materials, 15 and nanoparticle (NP) PEGylation to facilitate mucosal delivery. 16

However, various highly selective membrane transport processes found in living systems are based on attractive yet transient interactions between macromolecular cargo and biological membrane barriers.¹⁷ For example, importins pass through the nuclear envelope via transient, low-affinity hydrophobic interactions with the phenylalanine-glycine domains of nuclear pore complexes (NPCs). 18,19 The unveiling of this unique transport mechanism has stimulated recent efforts in incorporating NPC-derived protein sequences to

develop biomaterials that replicate NPC functions.²⁰⁻²⁴ In contrast to these biological transport systems, which have been optimized through evolution, synthetic transport systems rarely exploit transient interactions to achieve selectivity, due to the difficulties associated with fine-tuning cargo-barrier interactions. 25,26

Therefore, we sought to design and synthesize a molecular transport platform where the cargo-barrier interactions can be systemically modulated. By studying this platform as a model system, we will learn how cargo-barrier interactions can fundamentally affect the transport process and identify specific regimes where transient interactions result in optimal transport selectivity. The knowledge gained would not only provide new insights into many chemical/biological processes that operate based on similar principles^{27,28} but also ultimately lead to new selective transport systems that potentially surpass the efficiency of existing ones. Specifically, we hypothesized that DNA-DNA interactions, which can be chemically programmed to achieve a wide range of binding strengths, could

Received: August 3, 2021 Published: October 6, 2021





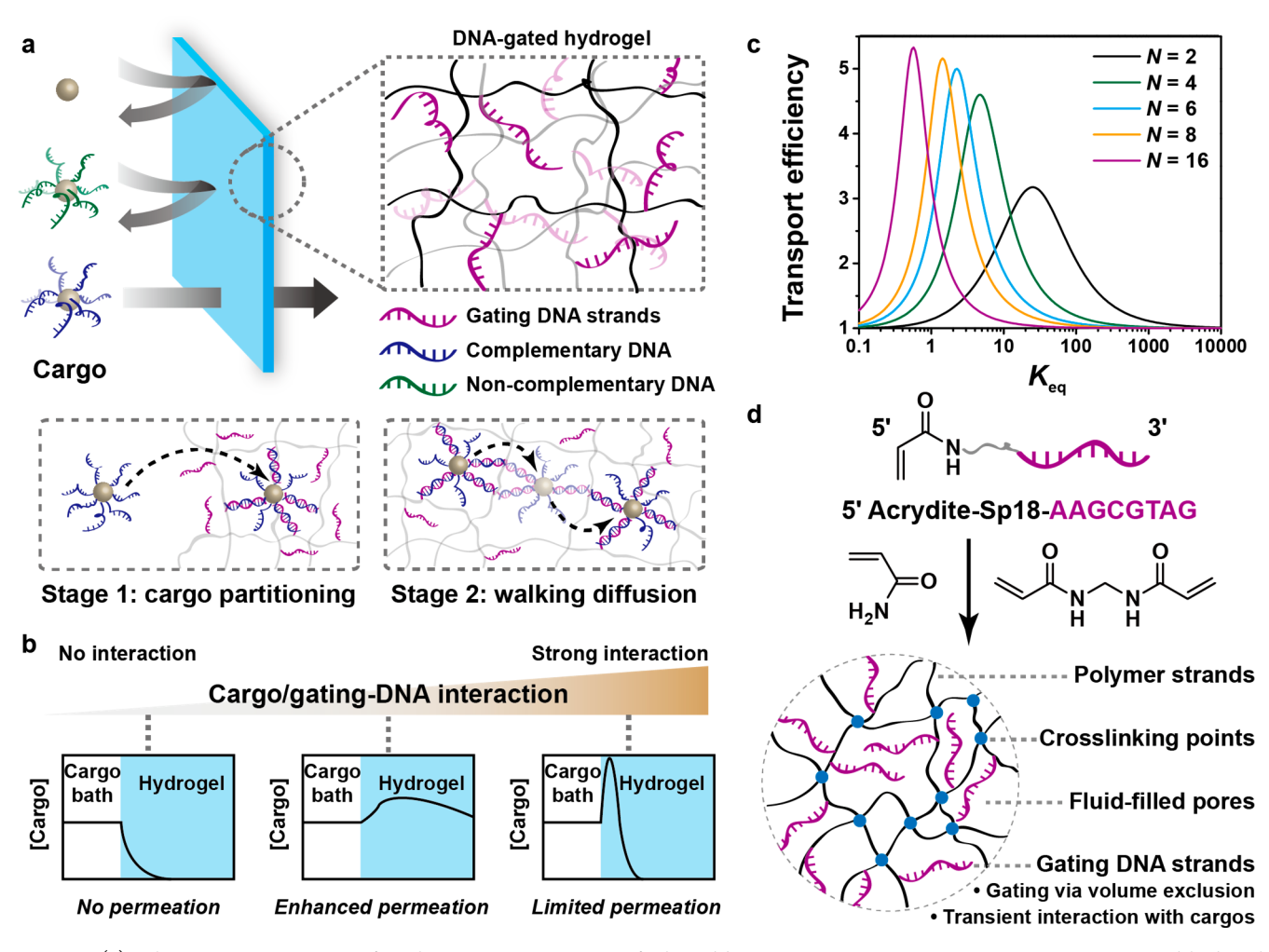


Figure 1. (a) Schematic representation of a selective transport process facilitated by transient DNA–DNA interactions. A DNA-gated hydrogel selectively transports cargo (e.g., small molecules, biomacromolecules, nanoparticles) bearing DNA sequences that are complementary to the gating DNA strands, provided that the DNA–DNA interaction is attractive enough to facilitate cargo partitioning into the hydrogel (Stage 1), yet sufficiently transient to allow the walking diffusion of cargo within the hydrogel (Stage 2). (b) The efficiency of this process is dictated by the cargo/gating-DNA interaction strength. Enhanced permeation can be achieved only with an intermediate cargo/gating-DNA interaction strength, where both Stage 1 and Stage 2 are favored. (c) Predicted binding strength dependence of the transport efficiency for cargo of various valencies. The results were calculated using binding-diffusion theory for a 10 nm cargo ([cargo] = 8 μ M) through a DNA-gated hydrogel ([DNA-gate] = 5 mM). $K_{\rm eq}$ is the binding constant between the gating DNA and the DNA on the cargo. N is the number of DNA strands on the cargo (i.e., cargo valency). Transport efficiency is defined as the flux ratio of DNA-tagged cargo to reference species of equal size that do not bind to the gating DNA strands. (d) Structures of the monomer, the cross-linker, and the gating DNA strand that are used to synthesize the DNA-gated hydrogel.

be leveraged to provide a promising route to selective transport systems based on transient cargo—barrier interactions. Importantly, surface DNA modification is a powerful strategy to introduce programmable DNA bonding interactions between molecules or NPs.^{29–32} Moreover, we recently discovered that, when small molecules or NPs with low DNA grafting density (i.e., fewer than 10 ssDNA per particle) are assembled with larger, complementary DNA-modified NPs (i.e., more than 160 ssDNA per particle) to form crystalline superlattices, the former become delocalized and diffusive in the lattice, effectively behaving as "electron equivalents" (EEs) in colloidal crystals.^{33,34} This observation supports the hypothesis that a binding regime may exist where efficient yet selective cargo transport can be achieved and DNA can be used to program cargo—barrier interactions.

Herein, we report a modular platform for selective cargo transport that is facilitated by DNA-DNA interactions. Specifically, a DNA-gated hydrogel was developed as the

transport barrier, where DNA strands were covalently incorporated into hydrogel pores^{35–37} to mediate the diffusion of nanoscopic species, resulting in a "gating" mechanism based on volume exclusion; 38-40 only cargo tagged with complementary DNA sequences may reversibly bind to these gating DNA strands and thus pass through the barrier (Figure 1a). We performed a theory-guided study to systematically examine how the DNA sequence and cargo valency (i.e., the number of DNA strands on the cargo) affected the transport processes, and we discovered a binding regime that leads to optimal transport selectivity. Furthermore, we synthesized a universal DNA-dendron transport tag for precise and convenient cargo modification, enabling bioinspired facilitated diffusion that is otherwise difficult to achieve and permitting a practical strategy for the selective transport of complex biomacromolecules in general.

■ RESULTS AND DISCUSSION

Designing a DNA-Gated Hydrogel Guided by Binding-Diffusion Theory. A cargo transport process through a membrane often involves two sequential steps-sorption and diffusion.²⁶ Hence, we divide the selective transport process in a DNA-gated hydrogel into two stages (Figure 1a, bottom): (1) the partitioning of cargo into the hydrogel facilitated by the affinity interactions between the gating DNA strands and cargo bearing complementary DNA sequences (Stage 1); (2) the repetitive de-hybridization and re-hybridization of the DNA strands on cargo with neighboring gating DNA strands, which results in a diffusion process akin to "walking" (Stage 2). The selectivity and efficiency of this two-stage transport process are primarily dictated by the cargo/gating-DNA interaction strength (Figure 1b). An insufficient cargo/gating-DNA affinity interaction would make Stage 1 unfavorable due to the volume and electrostatic exclusion imposed by the gating strands and lead to hindered cargo diffusion. On the other hand, although a strong cargo/gating-DNA interaction can selectively enrich cargo at the sol-gel interface, it significantly raises the energy barrier for Stage 2 and limits cargo permeation. Therefore, the initial goal was to identify an intermediate binding regime where the cargo/gating-DNA interaction is favorable yet transient such that both Stage 1 and Stage 2 will occur efficiently.

We began by calculating cargo diffusion in the context of 1D transport through a DNA-gated hydrogel using bindingdiffusion theory (see details in Supporting Information (SI), Section 1).⁴¹ In this model, DNA-tagged cargo is considered as a multivalent construct bearing N (i.e., cargo valency) sticky arms that each can reversibly bind to the gating DNA strands. This multivalency leads to a series of bound states varying the number of sticky arms that remain hybridized to the hydrogel.42 The equilibrium concentrations of these bound states are dictated by the binding constant (K_{eq}) between the gating DNA and the DNA on the cargo. The bound-state diffusivities were calculated and integrated into Fickian diffusion equations to solve for the transport efficiency, which was defined as the flux ratio of DNA-tagged cargo to equally sized reference species that do not bind to the gating DNA strands. Specifically, the diffusion of a 10 nm cargo ([cargo] = 8 μ M) through a DNA-gated hydrogel ([gating DNA] = 5 mM) was modeled (Figure 1c). The results suggest that theoretical binding regimes exist where optimal transport efficiencies can be achieved. While the locations of such regimes are valency-dependent, calculations provided numerical estimates that guided the experimental design. For cargo of intermediate valency (i.e., N = 4 to 16), the optimal transport efficiency was predicted to be when $K_{\rm eq}$ was between 0.5 and 5, which is typically observed for binding between short complementary DNA sequences that are no more than 8 base pairs (bps) long.⁴³

To experimentally access these binding regimes predicated by the model, we designed and synthesized an acrydite-terminated DNA strand bearing a flexible hexaethylene glycol phosphate spacer (Sp18) and a 5'-AAGCGTAG-3' sequence that allows for DNA-DNA hybridization of up to 8 bps (Figure 1d). After copolymerization with acrylamide (5 wt%) and *N,N'*-methylenebis(acrylamide) (0.15 wt%), the DNA strands (5 mM) were incorporated into a polyacrylamide hydrogel to gate the pores via volume exclusion. The monomer and cross-linker concentrations were chosen such that the

hydrogel mesh size was ~ 10 nm (see SI, Section 3, for a detailed discussion on the hydrogel mesh size), 44,45 large enough to permit the efficient transport of common macromolecular cargo but small enough so that the pores can be gated efficiently by the gating DNA strands.

Transport of DNA-Tagged AuNP Cargo: Binding Strength versus Transport Selectivity. Binding-diffusion theory identified K_{eq} and N as two critical parameters dictating the selective transport process. Therefore, we first examined how the DNA-DNA interaction strength would affect transport efficiency. To this end, 1.4 nm AuNPs were chosen as cargo for two reasons: (1) they can be conveniently functionalized with DNA ligands through thiol-gold interactions; (2) similar constructs have been shown to be diffusive in DNA-mediated colloidal superlattices by forming the desired transient interactions with complementary DNA strands (vide supra).33 We synthesized a series of thiolmodified DNA strands, each bearing a cyanine dye and a distinct 8-base sequence with tunable binding strength to the gating DNA (Figure 2a). They were used to functionalize 1.4 nm AuNPs to yield a series of conjugates denoted as AuNP-Pi (see synthetic details in SI, Section 4), where i indicates the number of complementary bases between the thiol-modified, NP surface-bound DNA and the gating DNA sequence in the hydrogel. These conjugates, which were prepared using a literature reported procedure to achieve an average valency of $N \approx 6.5^{33}$ were used as model cargo to be transported through a DNA-gated hydrogel barrier.

We performed transport experiments in a simplified 1D scenario, where a cargo solution reservoir ([cargo] = 8 μ M) was added to the exposed interface of a DNA-gated hydrogel prepared in a capillary tube (see details in SI, Section 3). The cargo transport through the hydrogel barrier was monitored by tracking the cyanine dye label using fluorescence microscopy. The solution volume was significantly larger than the hydrogel volume so the cargo concentration in the reservoir was considered constant, and the fluorescence intensity of the cargo solution was used as an internal reference. In each experiment, a Cy3-labeled AuNP-Pi (i = 3-7) solution was added to the hydrogel interface, and the cargo was allowed to diffuse for 24 h at a constant salt concentration (300 mM NaCl). The observed transport results (Figure 2b) followed the three scenarios that we presented in Figure 1b. The desired efficient cargo transport over a long diffusion distance was only achieved in the case of AuNP-P5 (corresponding to the middle scenario, Figure 1b). In contrast, weakly binding cargo (e.g., AuNP-P3 and AuNP-P4) exhibited limited partitioning to the hydrogel (corresponding to the left scenario, Figure 1b), while significant interfacial enrichment yet poor penetration was observed for strongly binding cargo (e.g., AuNP-P6 and AuNP-P7) (corresponding to the right scenario, Figure 1b). This trend can be clearly seen from fluorescence intensity profiles normalized to reservoir intensity (Figure 2c). On the other hand, all of the AuNP cargo were equally permeable in a DNA-free polyacrylamide hydrogel prepared at the same monomer and cross-linker concentrations (SI, Figure S3), suggesting that the DNA-gated hydrogel functioned as a selective transport barrier based on DNA-DNA interactions. Moreover, since we designed the system such that the cargo concentration (8 μ M) is significantly lower than the concentration of the covalent cross-linking points (10 mM), cargo transport has little effect on the mechanical properties of

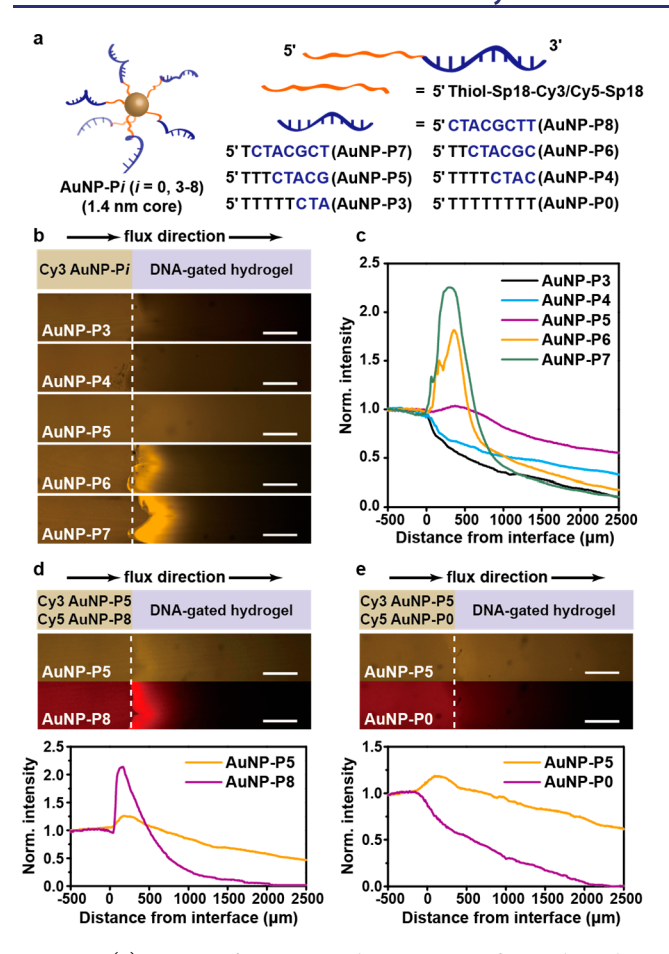


Figure 2. (a) Design of DNA-tagged AuNP cargo for studying how the DNA-DNA interaction strength affects the transport efficiency. DNA sequences that are complementary to the gating DNA are highlighted in blue. (b) Capillary transport results of Cy3-labeled AuNP-Pi (i = 3-7) through the DNA-gated hydrogel at 300 mM NaCl. Fluorescence microscopy images were taken 24 h after the cargo solutions (8 μ M) were added to one side of the hydrogels. (c) Fluorescence intensity profiles extracted from the fluorescence microscopy images in (b). Both (b) and (c) suggest that efficient transport over a long diffusion distance was only achieved with AuNP-P5. (d) Capillary transport results of Cy3-labeled AuNP-P5 and Cy5labeled AuNP-P8 and (e) Cy3-labeled AuNP-P5 and Cy5-labeled AuNP-P0 through the DNA-gated hydrogel at 300 mM NaCl. Fluorescence microscopy images were taken 24 h after the cargo solution (containing 8 μ M AuNP-P5 and 8 μ M AuNP-P8 or 8 μ M AuNP-P5 and 8 μ M AuNP-P0, respectively) was added to one side of the hydrogels. All scale bars are 500 μ m. The sol-gel interfaces are indicated by the dashed lines. Each intensity profile is normalized to the corresponding cargo reservoir intensity.

the DNA-gated hydrogel despite the potential formation of additional transient cross-linking points (SI, Figure S6).

Taking advantage of the sequence specificity of DNA-DNA interactions, we designed this selective transport system to operate efficiently in the presence of multiple cargo. For example, when a solution containing Cy3-labeled AuNP-PS and Cy5-labeled AuNP-P8 was used, the DNA-gated hydrogel selectively allowed AuNP-P5 to pass through while intercepting AuNP-P8 at the sol-gel interface (Figure 2d). The selectivity was also achieved with AuNP-P5 in the presence of AuNP-P0 cargo (Figure 2e). Since we designed the different cargo to have identical size and valency, the observed transport

selectivity was likely due to their differing binding interactions with the gating DNA.

The strength of DNA–DNA interactions increases as a function of increasing salt concentration. Thus, we performed AuNP-P5 transport experiments at various NaCl concentrations (0, 150, 300, and 500 mM). The data (SI, Figure S5) show that weaker DNA–DNA interactions at 0 mM NaCl indeed led to limited cargo partitioning to the DNA-gated hydrogel. Efficient cargo transport was achieved at the intermediate salt concentrations (150 and 300 mM NaCl), while a further increase in the salt concentration (500 mM NaCl) resulted in cargo–barrier interactions too strong to facilitate cargo penetration through the hydrogel. Taken together, investigations on AuNP cargo have enabled us to determine an experimentally accessible DNA–DNA binding regime, specific to 5-bp complementary regions for $N\approx 6.5$ cargo, where selective cargo transport can be achieved.

After establishing an understanding of cargo transport in the DNA-gated hydrogel, we incorporated 8 μ M of Cy3-labeled AuNP-Pi (i = 3, 5, 7) into the DNA-gated hydrogels prior to gelation to study cargo release from the hydrogel into an empty buffer bath using fluorescence microscopy. While a considerable amount of AuNP-P5 was released in 12 h, AuNP-P3 and AuNP-P7 showed only limited to moderate release during the same time frame (SI, Figure S7). In the case of AuNP-P3, we hypothesize that its weak interaction with the gating DNA strands is insufficient to open the gates. On the other hand, AuNP-P7 interacts strongly with the gating DNA such that it gets trapped in the hydrogel. Therefore, these results suggest a close correlation between cargo transport within the hydrogel and cargo release from the hydrogel. It is possible to facilitate both processes through judicious system design.

Cargo transport efficiency in the DNA-gated hydrogel also depends on the concentration of the gating DNA strands. For a specific cargo (e.g., $K_{eq} = 2$ and N = 6), this relationship can be predicted by binding-diffusion theory (SI, Figure S8), and three regimes are observed: (1) when the gating DNA concentration is low (e.g., below 0.1 mM), the DNA-gated hydrogel remains impenetrable to the cargo because there are insufficient numbers of binding sites; (2) at intermediate DNA concentrations (between 0.1 mM and 25 mM), cargo transport efficiency increases with the gating DNA concentration; and (3) at high gating DNA concentrations (above 25 mM), cargo transport efficiency plateaus as the number of available binding sites saturates in the hydrogel. Guided by these results, we studied the transport efficiency of AuNP-P5 in DNA-gated hydrogels prepared at four different gating DNA concentrations (0.1, 5, 25, and 50 mM), and we discovered a trend consistent with the theoretical prediction (SI, Figure S9). For the rest of this study, the gating DNA concentration was kept at 5 mM to achieve sufficient cargo transport at minimal gating DNA loading.

Transport of Small-Molecule–DNA Hybrids: Valency versus Transport Selectivity. Next, we studied the valency dependence of the selective transport process using cargo of various valencies (Figure 3a). At a constant DNA–DNA interaction strength (e.g., $K_{\rm eq}=2$), binding-diffusion theory predicts that the transport efficiency increases with N before reaching its maximum between N=6 and N=7. Initially, additional sticky arms favor the walking diffusion of cargo, but there comes a point where a further increase in N raises the energy barrier for each walking step due to increasing

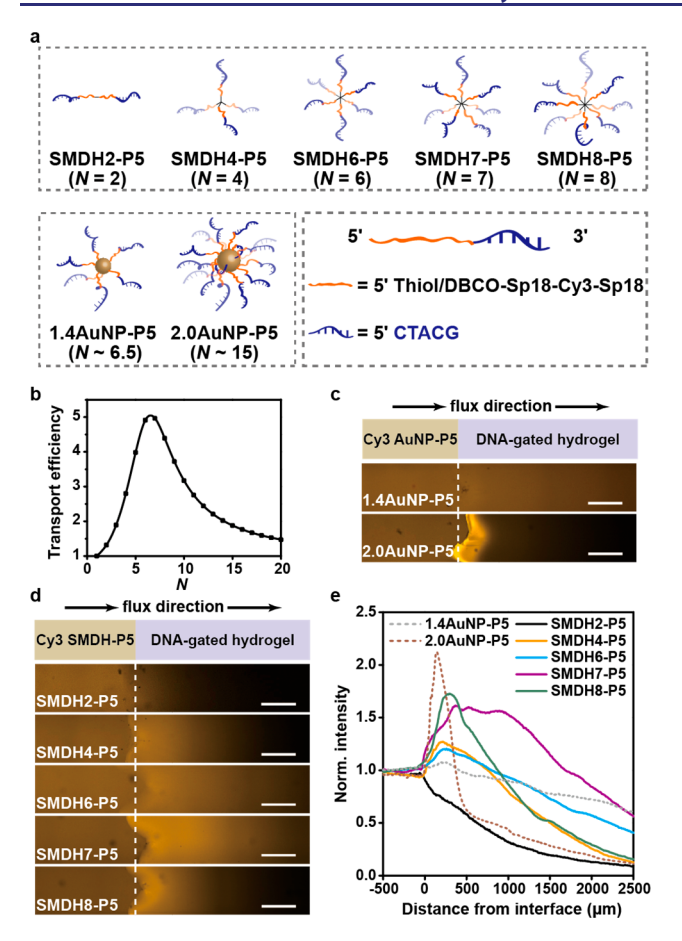


Figure 3. (a) Design of a series of SMDHs and two AuNP cargo for studying how cargo valency affects transport efficiency. (b) Predicted valency dependence of the transport efficiency at a constant DNA-DNA interaction strength ($K_{\rm eq}$ = 2). The results were calculated using binding-diffusion model for a 10 nm cargo ([cargo] = $8 \mu M$) through a DNA-gated hydrogel ([DNA-gate] = 5 mM). (c, d) Capillary transport results of the two Cy3-labeled AuNP-P5 (c) and various SMDHN-P5 (N = 2, 4, 6-8) (d) through the DNA-gated hydrogel at 300 mM NaCl. Fluorescence microscopy images were taken 24 h after the cargo solutions (8 μ M) were added to one side of the hydrogels. All scale bars are 500 μ m. The sol-gel interfaces are indicated by the dashed lines. (e) Fluorescence intensity profiles extracted from the fluorescence microscopy images in (c) and (d). Each intensity profile is normalized to the corresponding cargo reservoir intensity.

cooperativity⁴⁶ and eventually immobilizes cargo, resulting in reduced transport efficiency (Figure 3b).

We synthesized a series of multi-azido molecules and conjugated them with dibenzocyclooctyne (DBCO)-modified DNA strands via copper-free "click" chemistry (see synthetic details in SI, Section 5) to yield small-molecule-DNA hybrids (SMDHs) denoted as SMDHN-P5 (N = 2, 4, 6-8), where Ncorresponds to the number of DNA strands on each conjugate (Figure 3a). 34,47,48 These molecularly defined SMDHs, each with a distinct yet precise valency, were synthesized with an identical DNA sequence that forms a 5-bp hybridized region with the gating DNA strands. In addition, the same DNA sequence was used to functionalize 1.4 nm AuNPs and 2.0 nm AuNPs, resulting in two conjugates (denoted as 1.4AuNP-P5 and 2.0AuNP-P5) that have average valency of $N \approx 6.5$ and N \approx 15, respectively (Figure 3a). The SMDHs, in combination with these two DNA-functionalized AuNPs, represent a series of model cargo that enabled us to investigate the contribution

of valency in this selective transport process over a wide range of N.

We first examined the two AuNP-P5 cargo in capillary transport experiments. While 1.4AuNP-P5 exhibited efficient transport behavior, a strong accumulation band at the hydrogel interface was observed for 2.0AuNP-P5 (Figure 3c,e). This striking difference supports the predicted notion that exceedingly high valency, which would immobilize cargo in the bound state, leads to poor permeation. A more systematic understanding was achieved from the transport results of the various SMDH cargo. While the low-valency cargo (e.g., SMDH2-P5) showed poor interfacial partitioning and the high-valency cargo (e.g., SMDH8-P5) showed limited penetration, the cargo of intermediate valency was selectively transported through the DNA-gated hydrogel, where the maximum efficiency was achieved in the case of SMDH6-P5 and SMDH7-P5 (Figure 3d,e). To corroborate the valency dependence of these results, we confirmed that such transport selectivity could not be achieved using hydrogels without gating DNA strands. Since their hydrodynamic diameters (4.5-8.5 nm; see details in SI, Section 13) are smaller than the hydrogel pore size, 1.4AuNP-P5, 2.0AuNP-P5, and the SMDH cargo all efficiently penetrated DNA-free hydrogels (SI, Figure S4).

Universal DNA-Dendron Tag for Selective Transport of Biomacromolecules. The aforementioned studies of AuNP and SMDH cargo have proven that transient DNA-DNA interactions are a promising route to developing highly selective transport systems. Now, an efficient strategy is required to functionalize cargo with DNA of a precise valency and sequence predetermined to have optimized binding strength to the gating DNA, in order to apply this approach to more practically relevant cargo that often possess complex structures. Inspired by how nature has evolved a ubiquitous nuclear localization sequence (NLS) to tag proteins for import into the cell nucleus, ⁴⁹ we developed a DNA dendron⁵⁰ as a universal tag for the selective transport of complex macromolecules (Figure 4a). This DNA dendron (denoted as D6-P5) was synthesized to have a six-branch geometry at the 5' end where each branch features a 5'-CTACG-3' sequence that forms a 5-bp hybridized region with the gating DNA and a reactive handle at its 3' end for functionalization of cargo (see the complete sequence in SI, Section 2). This design was guided by the transport results of SMDH cargo (Figure 3e) and resulted in a transport tag that is highly permeable through the DNA-gated hydrogel (Figure 4b, top).

We evaluated this tagging strategy in the context of selective biomolecular transport. A green fluorescent protein, mNeon-Green (mNG),⁵¹ was chosen as the cargo because its intrinsic fluorescence allows us to easily track and understand the diffusion process. Upon expressing a cysteine mutation on the mNG surface, we were able to install a 3' thiol-modified Cy3labeled D6-P5 tag via disulfide exchange to yield a mNG-D6-P5 conjugate of high purity (see synthetic details in SI, Section 11). While the untagged mNG showed limited penetration through the hydrogel barrier due to the volume exclusion by the gating DNA strands (Figure 4b, bottom), mNG-D6-P5 was transported highly efficiently as evidenced by fluorescence imaging of both the mNG and Cy3 channels (Figure 4c,d). In contrast, enhanced transport was not observed when mNG was functionalized with D6-P0 (SI, Figure S11), which was synthesized by replacing the 5'-CTACG-3' region in D6-P5 with 5'-TTTTT-3' (see the complete sequence in SI, Section 2) to create a region that does not bind to the gating DNA

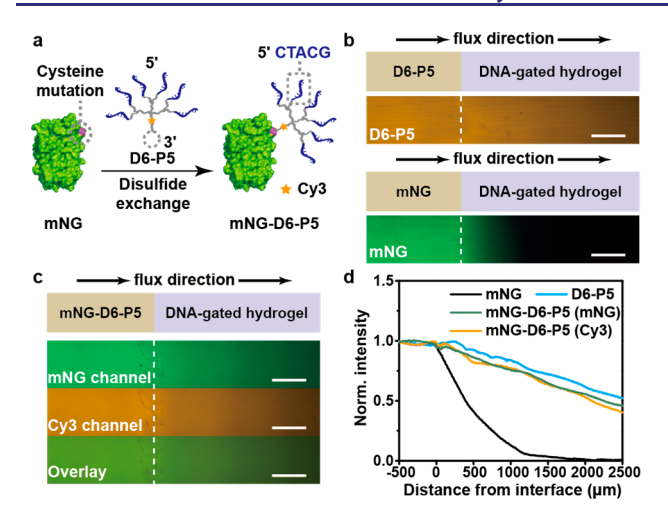


Figure 4. (a) Structure of a universal DNA-dendron transport tag (D6-P5) and its use in functionalizing mNeonGreen (mNG) via disulfide exchange. (b, c) Capillary transport results of D6-P5 (b, top), mNG (b, bottom), and mNG-D6-P5 (c) through the DNA-gated hydrogel at 300 mM NaCl. Fluorescence microscopy images were taken 24 h after the cargo solutions (8 μ M) were added to one side of the hydrogels. All scale bars are 500 μ m. The sol—gel interfaces are indicated by the dashed lines. (d) Fluorescence intensity profiles extracted from the fluorescence microscopy images in (b) and (c). Each intensity profile is normalized to the corresponding cargo reservoir intensity.

strands. We therefore conclude that D6-P5 facilitates protein transport through specific binding interactions with the gating DNA, rather than by simply modifying the protein surface charge distribution. Notably, although the dendron functionalization changes the hydrodynamic diameter of mNG from 5.4 to 8.5 nm (SI, Table S4), the transient DNA-DNA interaction provides a sufficiently strong driving force to offset this size increase, which would typically be unfavorable in the context of cargo transport. Furthermore, the DNA-dendron tagging strategy only requires one reactive site on complex structures and thus can be universally applied to a variety of macromolecular cargo. This novel strategy provides a new approach to controlling biomacromolecular transport, which is important yet challenging to achieve in applications involving, for example, the sustained release of macromolecular drugs or probes.2

Bioinspired Facilitated Transport Enabled by the DNA-Dendron Tag. In comparison to synthetic transport systems, those found in living cells, which operate in a crowded environment densely populated with a variety of other macromolecular species, possess a greater level of complexity that is often realized by integrating multiple specific binding interactions of different strengths. ^{17,54,55} For example, kinesinfacilitated cargo transport along microtubules involves a strong cargo—kinesin association for cargo loading, in combination with transient interactions between kinesin and tubulin subunits for cargo movement. ⁵⁶ Given the modularity and specificity of DNA—DNA interactions, we hypothesized that a similarly complex facilitated transport process could be achieved using the DNA-dendron tagging strategy.

Thus, we synthesized two DNA-dendron constructs as a cargo—transporter pair (Figure 5a,b, see complete sequences in SI, Section 2). Dendron A (i.e., the transporter) has a six-branched 5'-CTACG-3' transport tag at the 5' end and an 18-base DNA cargo receptor sequence at the 3' end. When the

Cy3-labeled Dendron A was added to one side of the DNAgated hydrogel, its transient interaction with the gating DNA strands effectively transported it to the other side of the barrier (Figure 5c). Dendron B (i.e., the cargo) contains a 3' recognition region that forms an 18-bp duplex with the receptor region of Dendron A, and a six-branched 5'-TTTTT-3' structure that does not bind with the gating DNA in the hydrogel barrier. Dendron B alone did not significantly penetrate the DNA-gated hydrogel (Figure 5d); however, we predicted that facilitated diffusion of Dendron B in the presence of Dendron A would occur due to the formation of a cargo-transporter complex (Figure 5b). Indeed, when the Cy3-labeled Dendron A and the Cy5-labeled Dendron B were separately added to opposite sides of the DNA-gated hydrogel, cargo transport occurred only after the Dendron A transporter reached the other side of the hydrogel to hybridize the Dendron B cargo (Figure 5e, after 48 h). After 72 h, the Dendron B cargo successfully reached the other side of the barrier (Figure 5e), indicative of facilitated transport processes. Interestingly, although the cargo-transporter complex (7.5 nm; SI, Table S4) has a larger hydrodynamic size than the transporter alone (5.4 nm; SI, Table S4), the former moves through the hydrogel at a similar rate as the latter alone (i.e., both took approximately 36 h to transport from one side to the other). While this result contradicts the conventional notion that size increase slows down cargo diffusion, it is reminiscent of the size independence of some biological facilitated transport processes.⁵⁷ For example, an importin can selectively bind to protein cargo up to 5 times its own size and facilitate cargo transport across nuclear pores at rates comparable to the nuclear transport rate of importin alone.⁵⁸ Therefore, the system reported herein is conceptually simple yet replicates many key features of biological transport processes, providing a potential strategy to overcome size limitations that are frequently encountered in synthetic transport systems.

While facilitated transport is widely present in nature, it has been challenging to realize synthetically, and success has been primarily limited to the facilitated diffusion of simple ions and small molecules. These results suggest that facilitated macromolecular diffusion can be achieved by combining multiple orthogonal DNA–DNA interactions in a single transport system. This bioinspired strategy features a general framework for facilitated transport, where one may leverage a high-affinity interaction for cargo recognition and a transient binding interaction for selective transport. In the future, this design principle may be generalized to systems involving other types of orthogonal interactions, with the potential of becoming a universal solution to facilitated macromolecular transport.

CONCLUSIONS

In this study, we leveraged DNA-DNA interactions as a new way of controlling the selective transport of macromolecular cargo and successfully demonstrated this concept using a DNA-gated hydrogel as the transport barrier. Taking advantage of the modularity of DNA-DNA interactions, we systematically examined how various aspects of cargo-barrier interactions (e.g., DNA-DNA binding strength, cargo valency) impact transport selectivity in a synthetic system for the first time. We used this platform to identify a regime where the specific cargo-barrier interaction is attractive enough to yield high selectivity, yet transient enough to allow efficient cargo transport. Building on these results, we utilized a DNA

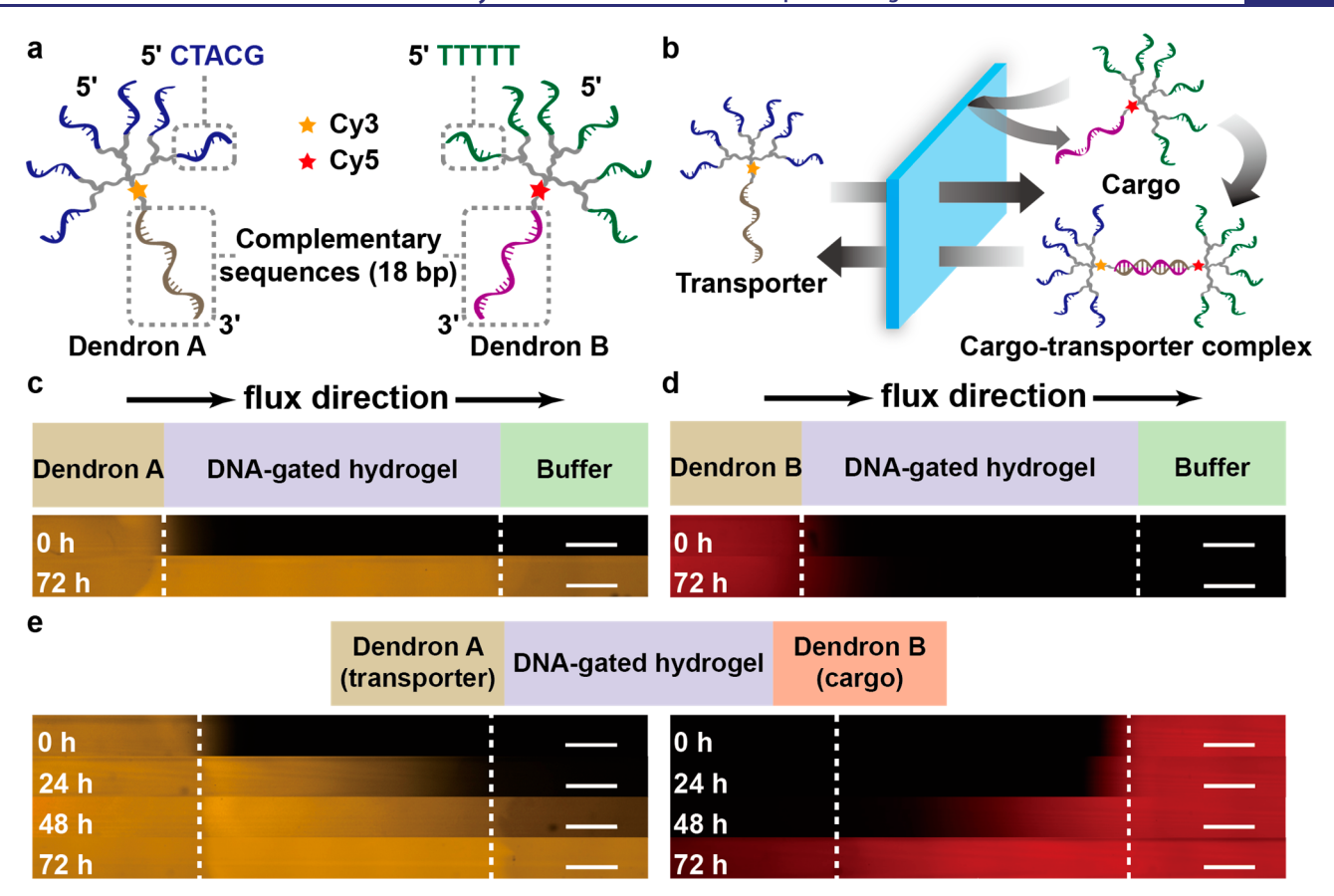


Figure 5. (a) Structures of two DNA dendrons acting as a cargo—transporter pair in a bioinspired facilitated transport process. (b) Schematic representation of the facilitated transport process. While the DNA-gated hydrogel hinders the transport of Dendron B (the cargo), it effectively transports Dendron A (the transporter) from one side to the other. Upon recognition by Dendron A via hybridization (18-bp), Dendron B can undergo facilitated diffusion in the form of a cargo—transporter complex. Capillary transport results of the (c) Cy3-labeled Dendron A (8 μ M) and (d) Cy5-labeled Dendron B (8 μ M) through the DNA-gated hydrogel at 300 mM NaCl. (e) Capillary transport results of a facilitated transport process where the Cy3-labeled Dendron A (8 μ M) and the Cy5-labeled Dendron B (8 μ M) were separately added to opposite sides of the DNA-gated hydrogel at 300 mM NaCl. Cargo transport occurred only after the transporter reached the other side to hybridize the cargo. All scale bars are 500 μ m. The sol—gel interfaces are indicated by the dashed lines.

dendron molecule as a universal transport tag, which can be conveniently functionalized onto macromolecular cargo to distinguish between target and non-target species, akin to how nature makes use of NLS to tag proteins for nuclear transport. Perhaps more impressively, the highly programmable nature of DNA—DNA interactions has enabled us to harmonize multiple orthogonal affinity interactions of different binding strengths to achieve a bioinspired facilitated transport process that has not been realized before in a synthetic macromolecular transport system.

Taken together, these results enhanced our basic understanding of how cargo—barrier interactions dictate cargo transport and allowed us to present a modular approach that has the potential to meet the demands of various emerging applications (e.g., sustained drug/probe release, \$2,53,60 complex reactions that take place in compartments, \$61,62 cell-signaling stimulation, \$63,64 and artificial cells \$65-67\$) involving selective macromolecular transport processes, where the level of complexity has exceeded what can be addressed by existing synthetic systems and thus requires fundamentally new solutions. For example, we envision that our transport strategy will provide a solution to the long-standing challenge of sustained insulin delivery. Subcutaneous implantation of a DNA-gated hydrogel encapsulating insulin—dendron conjugates will allow insulin release over extended periods of time,

where the release kinetics can be easily tuned by adjusting the DNA design. Moreover, the dendron tag may increase the stability of insulin while still allowing it to retain its bioactivity.

Moving forward, drawing on the rich literature of DNA designs that lead to diverse properties, this platform could be adapted to achieve more sophisticated transport systems. For example, stimuli-responsive DNA⁶⁸ could be used to achieve field-mediated directional transport processes. More importantly, while we chose a DNA-gated hydrogel to demonstrate selective transport at the microscale, this transport strategy and the DNA design principles should be readily applicable to other scaffolds, enabling similar processes at the nano- or macroscale.

ASSOCIATED CONTENT

Supporting Information

The Supporting Information is available free of charge at https://pubs.acs.org/doi/10.1021/jacs.1c08114.

Experimental procedures, modeling, additional transport results and fluorescence microscopy images, and DLS data (PDF)

AUTHOR INFORMATION

Corresponding Author

Chad A. Mirkin — Department of Chemistry and International Institute for Nanotechnology, Northwestern University, Evanston, Illinois 60208-3113, United States; orcid.org/0000-0002-6634-7627; Email: chadnano@northwestern.edu

Authors

- Yuwei Gu Department of Chemistry and International Institute for Nanotechnology, Northwestern University, Evanston, Illinois 60208-3113, United States; ⊚ orcid.org/0000-0002-9604-7764
- Max E. Distler Department of Chemistry and International Institute for Nanotechnology, Northwestern University, Evanston, Illinois 60208-3113, United States; orcid.org/0000-0002-3750-5075
- Ho Fung Cheng Department of Chemistry and International Institute for Nanotechnology, Northwestern University, Evanston, Illinois 60208-3113, United States; orcid.org/0000-0003-2580-0912
- Chi Huang Department of Chemistry and International Institute for Nanotechnology, Northwestern University, Evanston, Illinois 60208-3113, United States

Complete contact information is available at: https://pubs.acs.org/10.1021/jacs.1c08114

Notes

The authors declare the following competing financial interest(s): C.A.M., Y.G., M.E.D., and H.F.C. are inventors on a U.S. patent application to be filed on this work.

■ ACKNOWLEDGMENTS

The authors acknowledge S. H. Petrosko and S. M. Rupich for providing editorial input, and Y. Yang for help with rheological measurements. This material is based upon work supported by the Air Force Office of Scientific Research under awards FA9550-17-1-0348 (oligonucleotide synthesis/purification and DNA-nanoparticle functionalization) and FA9550-18-1-0493 (confocal imaging of transport processes), the National Science Foundation under grant CHE-1709888 (synthesis of small-molecule-DNA hybrids), and the Sherman Fairchild Foundation, Inc. (transport modeling). It was also supported as part of the Center for Bio-Inspired Energy Science, an Energy Frontier Research Center funded by the U.S. Department of Energy, Office of Science, Basic Energy Sciences under award DE-SC0000989 (synthesis of protein-DNA conjugates). This work made use of instruments of IMSERC at Northwestern University that have received support from the Soft and Hybrid Nanotechnology Experimental (SHyNE) Resource (NSF ECCS-1542205), the State of Illinois, and the International Institute for Nanotechnology (IIN). C.H. acknowledges the Chinese Scholarship Council (CSC) for funding support (201906130213).

REFERENCES

- (1) Peppas, N. A.; Khare, A. R. Preparation, structure and diffusional behavior of hydrogels in controlled release. *Adv. Drug Delivery Rev.* **1993**, *11*, 1–35.
- (2) Lin, C.-C.; Anseth, K. S. PEG Hydrogels for the Controlled Release of Biomolecules in Regenerative Medicine. *Pharm. Res.* **2009**, 26, 631–643.

- (3) Fu, Y.; Kao, W. J. Drug release kinetics and transport mechanisms of non-degradable and degradable polymeric delivery systems. *Expert Opin. Drug Delivery* **2010**, *7*, 429–444.
- (4) Rehmann, M. S.; Skeens, K. M.; Kharkar, P. M.; Ford, E. M.; Maverakis, E.; Lee, K. H.; Kloxin, A. M. Tuning and Predicting Mesh Size and Protein Release from Step Growth Hydrogels. *Biomacromolecules* **2017**, *18*, 3131–3142.
- (5) Bohn, P. W. Nanoscale Control and Manipulation of Molecular Transport in Chemical Analysis. *Annu. Rev. Anal. Chem.* **2009**, *2*, 279–296.
- (6) Restrepo-Pérez, L.; Joo, C.; Dekker, C. Paving the way to single-molecule protein sequencing. *Nat. Nanotechnol.* **2018**, *13*, 786–796.
- (7) Chmelik, C.; Kärger, J. In situ study on molecular diffusion phenomena in nanoporous catalytic solids. *Chem. Soc. Rev.* **2010**, 39, 4864–4884.
- (8) Johnson, B. A.; Beiler, A. M.; McCarthy, B. D.; Ott, S. Transport Phenomena: Challenges and Opportunities for Molecular Catalysis in Metal—Organic Frameworks. *J. Am. Chem. Soc.* **2020**, *142*, 11941—11956.
- (9) Yang, T.; Lin, H.; Loh, K. P.; Jia, B. Fundamental Transport Mechanisms and Advancements of Graphene Oxide Membranes for Molecular Separation. *Chem. Mater.* **2019**, *31*, 1829–1846.
- (10) Cheng, L.; Liu, G.; Zhao, J.; Jin, W. Two-Dimensional-Material Membranes: Manipulating the Transport Pathway for Molecular Separation. *Acc. Mater. Res.* **2021**, *2*, 114–128.
- (11) Liu, X.; Bruening, M. L. Size-Selective Transport of Uncharged Solutes through Multilayer Polyelectrolyte Membranes. *Chem. Mater.* **2004**, *16*, 351–357.
- (12) Assen, A. H.; Belmabkhout, Y.; Adil, K.; Bhatt, P. M.; Xue, D.-X.; Jiang, H.; Eddaoudi, M. Ultra-Tuning of the Rare-Earth fcu-MOF Aperture Size for Selective Molecular Exclusion of Branched Paraffins. *Angew. Chem., Int. Ed.* **2015**, *54*, 14353–14358.
- (13) Porter, C. J.; Werber, J. R.; Zhong, M.; Wilson, C. J.; Elimelech, M. Pathways and Challenges for Biomimetic Desalination Membranes with Sub-Nanometer Channels. *ACS Nano* **2020**, *14*, 10894–10916.
- (14) Young, C. L.; Britton, Z. T.; Robinson, A. S. Recombinant protein expression and purification: A comprehensive review of affinity tags and microbial applications. *Biotechnol. J.* **2012**, *7*, 620–634
- (15) Alsbaiee, A.; Smith, B. J.; Xiao, L.; Ling, Y.; Helbling, D. E.; Dichtel, W. R. Rapid removal of organic micropollutants from water by a porous β -cyclodextrin polymer. *Nature* **2016**, *529*, 190–194.
- (16) Huckaby, J. T.; Lai, S. K. PEGylation for enhancing nanoparticle diffusion in mucus. *Adv. Drug Delivery Rev.* **2018**, *124*, 125–139.
- (17) Lieleg, O.; Ribbeck, K. Biological hydrogels as selective diffusion barriers. *Trends Cell Biol.* **2011**, *21*, 543–551.
- (18) Cook, A.; Bono, F.; Jinek, M.; Conti, E. Structural Biology of Nucleocytoplasmic Transport. *Annu. Rev. Biochem.* **200**7, *76*, 647–
- (19) Knockenhauer, K. E.; Schwartz, T. U. The Nuclear Pore Complex as a Flexible and Dynamic Gate. *Cell* **2016**, *164*, 1162–1171.
- (20) Frey, S.; Görlich, D. A Saturated FG-Repeat Hydrogel Can Reproduce the Permeability Properties of Nuclear Pore Complexes. *Cell* **2007**, *130*, 512–523.
- (21) Bird, S. P.; Baker, L. A. An Abiotic Analogue of the Nuclear Pore Complex Hydrogel. *Biomacromolecules* **2011**, *12*, 3119–3123.
- (22) Kim, M.; Chen, W. G.; Kang, J. W.; Glassman, M. J.; Ribbeck, K.; Olsen, B. D. Artificially Engineered Protein Hydrogels Adapted from the Nucleoporin Nsp1 for Selective Biomolecular Transport. *Adv. Mater.* **2015**, *27*, 4207–4212.
- (23) Maguire, L.; Betterton, M. D.; Hough, L. E. Bound-State Diffusion due to Binding to Flexible Polymers in a Selective Biofilter. *Biophys. J.* **2020**, *118*, 376–385.
- (24) Yang, Y. J.; Mai, D. J.; Li, S.; Morris, M. A.; Olsen, B. D. Tuning Selective Transport of Biomolecules through Site-Mutated Nucleoporin-like Protein (NLP) Hydrogels. *Biomacromolecules* **2021**, *22*, 289–298.

- (25) Matile, S.; Vargas Jentzsch, A.; Montenegro, J.; Fin, A. Recent synthetic transport systems. *Chem. Soc. Rev.* **2011**, *40*, 2453–2474.
- (26) Sujanani, R.; Landsman, M. R.; Jiao, S.; Moon, J. D.; Shell, M. S.; Lawler, D. F.; Katz, L. E.; Freeman, B. D. Designing Solute-Tailored Selectivity in Membranes: Perspectives for Water Reuse and Resource Recovery. *ACS Macro Lett.* **2020**, *9*, 1709–1717.
- (27) Frey, S.; Richter, R. P.; Görlich, D. FG-Rich Repeats of Nuclear Pore Proteins Form a Three-Dimensional Meshwork with Hydrogel-Like Properties. *Science* **2006**, *314*, 815–817.
- (28) Rapp, P. B.; Omar, A. K.; Silverman, B. R.; Wang, Z.-G.; Tirrell, D. A. Mechanisms of Diffusion in Associative Polymer Networks: Evidence for Chain Hopping. *J. Am. Chem. Soc.* **2018**, *140*, 14185–14194.
- (29) Mirkin, C. A.; Letsinger, R. L.; Mucic, R. C.; Storhoff, J. J. A DNA-based method for rationally assembling nanoparticles into macroscopic materials. *Nature* **1996**, *382*, 607–609.
- (30) Macfarlane, R. J.; O'Brien, M. N.; Petrosko, S. H.; Mirkin, C. A. Nucleic Acid-Modified Nanostructures as Programmable Atom Equivalents: Forging a New "Table of Elements. *Angew. Chem., Int. Ed.* **2013**, *52*, *5688*–*5698*.
- (31) Jones, M. R.; Seeman, N. C.; Mirkin, C. A. Programmable materials and the nature of the DNA bond. *Science* **2015**, 347, 1260901.
- (32) Laramy, C. R.; O'Brien, M. N.; Mirkin, C. A. Crystal engineering with DNA. *Nat. Rev. Mater.* **2019**, *4*, 201–224.
- (33) Girard, M.; Wang, S.; Du, J. S.; Das, A.; Huang, Z.; Dravid, V. P.; Lee, B.; Mirkin, C. A.; Olvera de la Cruz, M. Particle analogs of electrons in colloidal crystals. *Science* **2019**, *364*, 1174–1178.
- (34) Cheng, H. F.; Wang, S.; Mirkin, C. A. Electron-Equivalent Valency through Molecularly Well-Defined Multivalent DNA. *J. Am. Chem. Soc.* **2021**, *143*, 1752–1757.
- (35) Kahn, J. S.; Hu, Y.; Willner, I. Stimuli-Responsive DNA-Based Hydrogels: From Basic Principles to Applications. *Acc. Chem. Res.* **2017**, *50*, 680–690.
- (36) Li, F.; Tang, J.; Geng, J.; Luo, D.; Yang, D. Polymeric DNA hydrogel: Design, synthesis and applications. *Prog. Polym. Sci.* **2019**, 98, 101163.
- (37) Gačanin, J.; Synatschke, C. V.; Weil, T. Biomedical Applications of DNA-Based Hydrogels. *Adv. Funct. Mater.* **2020**, *30*, 1906253.
- (38) Buchsbaum, S. F.; Nguyen, G.; Howorka, S.; Siwy, Z. S. DNA-Modified Polymer Pores Allow pH- and Voltage-Gated Control of Channel Flux. J. Am. Chem. Soc. 2014, 136, 9902–9905.
- (39) Li, P.; Xie, G.; Kong, X.-Y.; Zhang, Z.; Xiao, K.; Wen, L.; Jiang, L. Light-Controlled Ion Transport through Biomimetic DNA-Based Channels. *Angew. Chem., Int. Ed.* **2016**, *55*, 15637–15641.
- (40) Wu, Y.; Wang, D.; Willner, I.; Tian, Y.; Jiang, L. Smart DNA Hydrogel Integrated Nanochannels with High Ion Flux and Adjustable Selective Ionic Transport. *Angew. Chem., Int. Ed.* **2018**, *57*, 7790–7794.
- (41) Yang, Y. J.; Mai, D. J.; Dursch, T. J.; Olsen, B. D. Nucleopore-Inspired Polymer Hydrogels for Selective Biomolecular Transport. *Biomacromolecules* **2018**, *19*, 3905–3916.
- (42) Ramirez, J.; Dursch, T. J.; Olsen, B. D. A Molecular Explanation for Anomalous Diffusion in Supramolecular Polymer Networks. *Macromolecules* **2018**, *51*, 2517–2525.
- (43) Menssen, R. J.; Tokmakoff, A. Length-Dependent Melting Kinetics of Short DNA Oligonucleotides Using Temperature-Jump IR Spectroscopy. *J. Phys. Chem. B* **2019**, *123*, 756–767.
- (44) Urueña, J. M.; Pitenis, A. A.; Nixon, R. M.; Schulze, K. D.; Angelini, T. E.; Gregory Sawyer, W. Mesh Size Control of Polymer Fluctuation Lubrication in Gemini Hydrogels. *Biotribology* **2015**, *1*–2, 24–29.
- (45) Bhattacharyya, A.; O'Bryan, C.; Ni, Y.; Morley, C. D.; Taylor, C. R.; Angelini, T. E. Hydrogel compression and polymer osmotic pressure. *Biotribology* **2020**, *22*, 100125.
- (46) Gibbs-Davis, J. M.; Schatz, G. C.; Nguyen, S. T. Sharp Melting Transitions in DNA Hybrids without Aggregate Dissolution: Proof of

- Neighboring-Duplex Cooperativity. J. Am. Chem. Soc. 2007, 129, 15535–15540.
- (47) Eryazici, I.; Prytkova, T. R.; Schatz, G. C.; Nguyen, S. T. Cooperative Melting in Caged Dimers with Only Two DNA Duplexes. J. Am. Chem. Soc. 2010, 132, 17068–17070.
- (48) Thaner, R. V.; Eryazici, I.; Farha, O. K.; Mirkin, C. A.; Nguyen, S. T. Facile one-step solid-phase synthesis of multitopic organic—DNA hybrids via "click" chemistry. *Chem. Sci.* **2014**, *5*, 1091–1096.
- (49) Kalderon, D.; Roberts, B. L.; Richardson, W. D.; Smith, A. E. A short amino acid sequence able to specify nuclear location. *Cell* **1984**, 39, 499–509.
- (50) Distler, M. E.; Teplensky, M. H.; Bujold, K. E.; Kusmierz, C. D.; Evangelopoulos, M.; Mirkin, C. A. DNA Dendrons as Agents for Intracellular Delivery. *J. Am. Chem. Soc.* **2021**, *143*, 13513–13518.
- (51) Shaner, N. C.; Lambert, G. G.; Chammas, A.; Ni, Y.; Cranfill, P. J.; Baird, M. A.; Sell, B. R.; Allen, J. R.; Day, R. N.; Israelsson, M.; Davidson, M. W.; Wang, J. A bright monomeric green fluorescent protein derived from Branchiostoma lanceolatum. *Nat. Methods* **2013**, *10*, 407–409.
- (52) Yu, M.; Wu, J.; Shi, J.; Farokhzad, O. C. Nanotechnology for protein delivery: Overview and perspectives. *J. Controlled Release* **2016**, 240, 24–37.
- (53) Awwad, S.; Angkawinitwong, U. Overview of Antibody Drug Delivery. *Pharmaceutics* **2018**, *10*, 83.
- (54) Tagliazucchi, M.; Szleifer, I. Transport mechanisms in nanopores and nanochannels: can we mimic nature? *Mater. Today* **2015**, *18*, 131–142.
- (55) Witten, J.; Ribbeck, K. The particle in the spider's web: transport through biological hydrogels. *Nanoscale* **2017**, *9*, 8080–8095.
- (56) Schimert, K. I.; Budaitis, B. G.; Reinemann, D. N.; Lang, M. J.; Verhey, K. J. Intracellular cargo transport by single-headed kinesin motors. *Proc. Natl. Acad. Sci. U. S. A.* **2019**, *116*, 6152–6161.
- (57) Ribbeck, K.; Görlich, D. Kinetic analysis of translocation through nuclear pore complexes. *EMBO J.* **2001**, 20, 1320–1330.
- (58) Panté, N.; Kann, M. Nuclear Pore Complex Is Able to Transport Macromolecules with Diameters of ~ 39 nm. *Mol. Biol. Cell* **2002**, *13*, 425–434.
- (59) Li, Y.; Wang, S.; He, G.; Wu, H.; Pan, F.; Jiang, Z. Facilitated transport of small molecules and ions for energy-efficient membranes. *Chem. Soc. Rev.* **2015**, *44*, 103–118.
- (60) Natarajan, J. V.; Nugraha, C.; Ng, X. W.; Venkatraman, S. Sustained-release from nanocarriers: a review. *J. Controlled Release* **2014**, 193, 122–138.
- (61) Tsitkov, S.; Hess, H. Design Principles for a Compartmentalized Enzyme Cascade Reaction. ACS Catal. 2019, 9, 2432–2439.
- (62) Xie, G.; Forth, J.; Chai, Y.; Ashby, P. D.; Helms, B. A.; Russell, T. P. Compartmentalized, All-Aqueous Flow-Through-Coordinated Reaction Systems. *Chem.* **2019**, *5*, 2678–2690.
- (63) Douglas, S. M.; Bachelet, I.; Church, G. M. A Logic-Gated Nanorobot for Targeted Transport of Molecular Payloads. *Science* **2012**, 335, 831–834.
- (64) Lai, J.; Li, S.; Shi, X.; Coyne, J.; Zhao, N.; Dong, F.; Mao, Y.; Wang, Y. Displacement and hybridization reactions in aptamer-functionalized hydrogels for biomimetic protein release and signal transduction. *Chem. Sci.* **2017**, *8*, 7306–7311.
- (65) Schmitt, C.; Lippert, A. H.; Bonakdar, N.; Sandoghdar, V.; Voll, L. M. Compartmentalization and Transport in Synthetic Vesicles. *Front. Bioeng. Biotechnol.* **2016**, *4*, 19.
- (66) Deng, N.-N.; Yelleswarapu, M.; Zheng, L.; Huck, W. T. S. Microfluidic Assembly of Monodisperse Vesosomes as Artificial Cell Models. *J. Am. Chem. Soc.* **2017**, *139*, 587–590.
- (67) Molla, M. R.; Rangadurai, P.; Antony, L.; Swaminathan, S.; de Pablo, J. J.; Thayumanavan, S. Dynamic actuation of glassy polymersomes through isomerization of a single azobenzene unit at the block copolymer interface. *Nat. Chem.* **2018**, *10*, 659–666.
- (68) Yu, Y.; Jin, B.; Li, Y.; Deng, Z. Stimuli-Responsive DNA Self-Assembly: From Principles to Applications. *Chem. Eur. J.* **2019**, 25, 9785–9798.